

# OPTICAL VARIABILITY OF THE BLAZAR 3C 454.3 DURING 2007-2010

V.A. Hagen-Thorn<sup>1</sup>, V.M. Larionov<sup>1,2</sup>, A.A. Arkharov<sup>1,2</sup>, E.I. Hagen-Thorn<sup>1,2</sup>, D.A. Blinov<sup>3,1</sup>

<sup>1</sup>Astronomical Institute of St.-Petersburg State University <sup>2</sup>Pulkovo Observatory <sup>3</sup>University of Crete

The optical variability of the blazar 3C 454.3 during 2007-2010 has been studied using the results of multicolor (*BVRJHK*) observations carried out in the Astronomical Institute of St.-Petersburg State University and Pulkovo Observatory. The existence of two variable synchrotron sources was found. The first is responsible for the flux variability of small amplitude, the second – for the flares. In each flare the relative SED of variable source was found to be constant but spectral indexes were different in different flares. This fact points to impossibility to explain the global variability *only* by geometrical reasons. The *observed* color variability is due to a superposition of the variable and constant components with different SEDs

## INTRODUCTION

The blazar 3C 454.3 is an optically active object at  $z = 0.859$ . The light curve for 1966–2005 presented in [1] shows that, prior to 2001, the object displayed moderate brightness variations between  $15^m$  and  $17^m$  in the *R* band. The activity then increased, and an unprecedented strong outburst was recorded in 2005 [2]; the brightness of the object reached  $R \approx 12^m$ . A detailed *R*-band light curve and *B*-*R* color curve for 2004.4–2005.8, covering the ascending (the brightness increase started at about 2004.65) and descending branches of the outburst, are presented in [1].

The interesting feature of the 2004–2005 outburst was that the object was redder when brighter. The opposite relation is observed for almost all active galactic nuclei, though the cases when an object became redder with increasing brightness have also been encountered earlier, for example, for the blazar 3C 345. A detailed analysis of color variations of 3C 345 [3, 4] have shown that a synchrotron component with constant relative SED and variable flux was responsible for the brightness variations. Its flux was combined with that of a bluer constant component (the blue bump). A similar qualitative explanation was suggested in [1] to explain the color behavior of 3C 454.3 during its outburst but the possibility of varying color characteristics of the variable component was noted. The behavior of the object in the 2004-2005 outburst and in post-eruptive stage (2006) was studied in [5] where the constancy of the relative SED of synchrotron component responsible for activity of 3C 454.3 was established and observed dependence between brightness and color of the object was explained.

In 2007-2010 several outbursts of 3C 454.3 were observed and here we give the results of detailed study of color variability of the object in this events (for some events the information on color variability may be found in [6, 7]).

## OBSERVATIONAL DATA AND METHOD OF ANALYSIS

Optical observations in optical (*B,V,R,I*) bands were carried out at two telescopes: 70-cm of Crimean Observatory and 40-cm of Astronomical Institute of St.-Petersburg State University. Both are equipped by identical CCD photometer-polarimeters. The observing and reduction techniques are described in [8]. The uncertainties of our photometric estimates ( $1\sigma$  level) are no more than 0.03<sup>m</sup>. The observations in the near-IR (*J, H, K*) bands were acquired with the 1.1-m telescope in Campo Imperatore (Italy) with SWIRCAM camera. The observation and reduction techniques are also described in [8]. The uncertainties of our individual IR brightness estimates are no more than 0.02<sup>m</sup>.

The technique that was used in our analysis of the color variations is described in [9]. It assumes the presence of two components in the radiation: one constant and one variable, with the latter responsible for the source activity. The main advantage of this technique is that the color characteristics of the variable component are derived directly from the observations, without preliminary determination of its contribution to the combined light, thus eliminating possible errors due to erroneous estimates of this contribution.

The technique, which has been used to analyze color variations of blazars many times (see, for instance, [5]), is based on plotting “flux-flux” diagrams for two bands (actually, flux densities are used, referred to as “fluxes” for the sake of brevity). The data for simultaneous observations lie along straight lines in such diagrams if the color characteristics of the variable component remain unchanged during the studied time interval; the slopes of these lines yield the flux ratios for the variable component in the analyzed bands. Thus, multicolor variability observations can provide the relative SED of the variable component.

It is convenient to derive the SED of the variable source separately in the optical and IR. These SEDs are then joined together using a flux-flux diagram for the fluxes in one of the optical bands and one of the IR bands.

In Fig. 1 we give the light curves of 3C 454.3 in *B,V,R,I,J,H,K* bands after transforming to fluxes via absolute calibration of Mead et al. [10] and averaging on given JD all estimates obtained in this night. By averaging data within a night, we neglect very fast variations, but their amplitude is small, and the procedure will have no influence on the results of our further analysis.

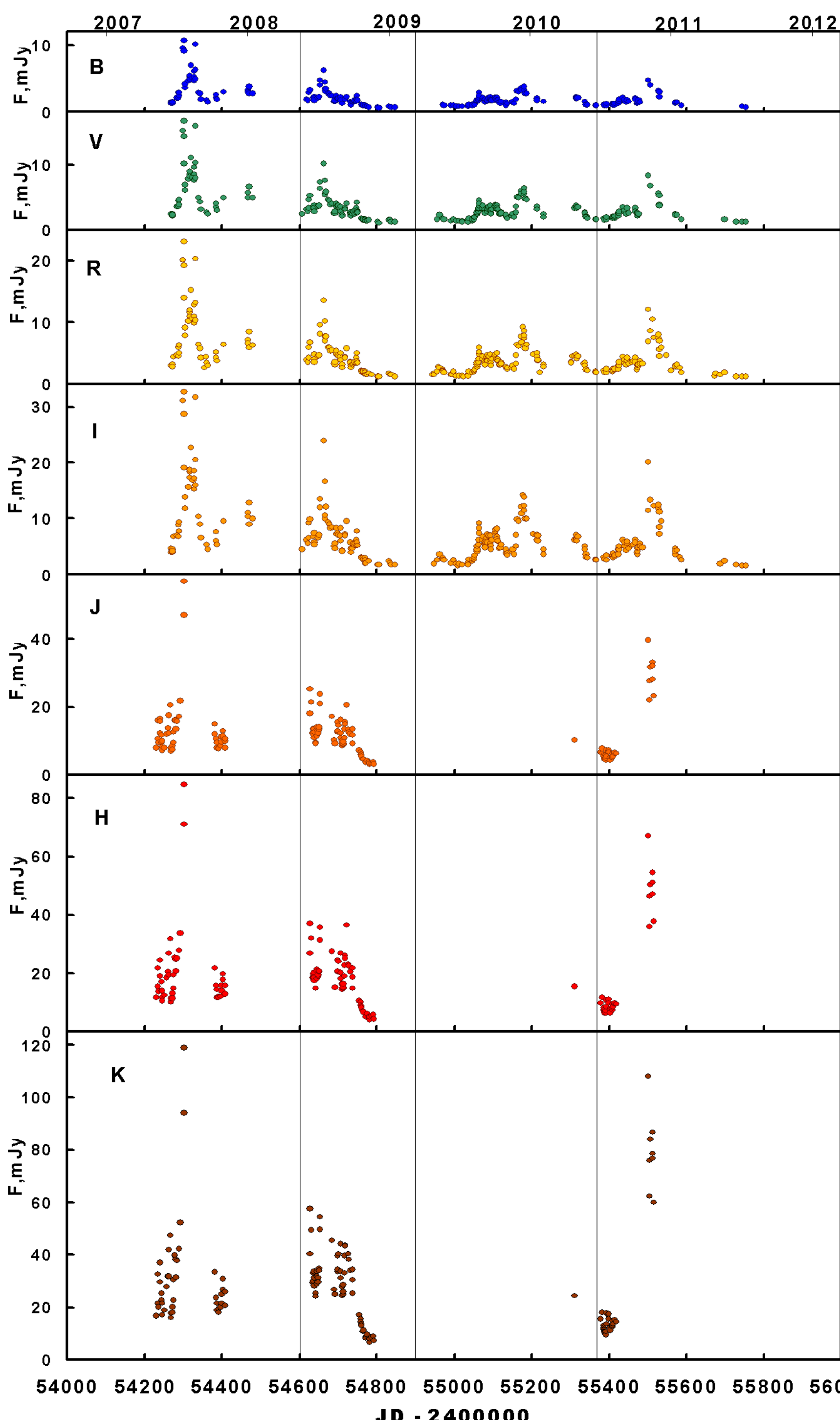


Fig.1. Light curves of 3C454.3 after transforming to fluxes and averaging on given JD all estimates obtained in this night.

## DISCUSSION AND CONCLUSIONS

First of all let us note that at flux-flux diagrams (Fig. 2) there are no systematic deviations from straight lines. This fact points to constancy at average of color characteristics of variable source responsible for activity. At the same time the small break may be noticed in the region near the upper boundary of smooth flux variations. The same situation was found for BL Lac in [13] and was explained by existence of two variable sources: the first one responsible for smooth variations and the second – for flares. Here we propose the same interpretation. The spectra of both sources are of power law. This fact and high observed polarization point to synchrotron nature of the sources. Their spectral indexes are essentially different (Fig. 4) thus confirming correctness of separation of the sources responsible for outbursts from the source responsible for smooth variations. The former sources have different SEDs (Fig. 5).

As a consequence we must refuse from an attempt to explain the global variability *only* by difference in Doppler boosting due to variations of angle between the line of sight and direction of electron moving. At the same time this mechanism seems to give the best explanation of the constancy of SED in each event that is most probably due to shock-wave moving along the curved jet or jet with helical magnetic field. The SED differences in different outbursts obviously reflect differences in the electron-energy distributions in the sources responsible for the outbursts.

In contrast to the spectrum of variable component the spectrum of constant component is not smooth (Fig. 3). There is extra radiation in bands *J* and *V*. These features in the case of low fluxes were noted via photometry in [6] and were explained as possible contribution of emission lines. Later on their existence was confirmed by spectral observations [14,15].

At Fig. 3 we give also corrected for interstellar absorption spectra for observed values  $F_R = 1$  mJy (asterisks),  $F_R = 2$  mJy (squares) и  $F_R = 20$  mJy (triangles), fluxes for other bands were found using equations (1). The first value is near to that of constant component, the second is by  $\approx 1^m$  brighter and the third is near to maximum observed flux. We see that for  $F_R = 1$  mJy the details in SED are well noticeable, but for  $F_R = 2$  mJy they are no longer detectable. The spectrum becomes bluer and follows the power law (with  $\alpha = -1.47 \pm 0.03$ ). For  $F_R = 20$  mJy we see the power-law spectrum with  $\alpha = -1.31 \pm 0.04$ . Just as one should expect this value is the same as found for the variable component ( $\alpha = -1.33 \pm 0.05$ ). Null-point at right ordinate axis at Fig. 3 has been chosen to emphasize this fact.

In conclusion, let us dwell on *observed* color variability of 3C 454.3. As we have shown in [5], the observed in 2004-2005 dependence between color and brightness (redder when brighter) is naturally explained by flux variations of very red synchrotron source (with  $\alpha = -1.82 \pm 0.04$ ) whose radiation was superposed on the radiation of bluer constant component. In 2007-2010 the situation is different. Synchrotron source responsible for variability was bluer ( $\alpha = -1.33 \pm 0.05$ ) than constant component so that the dependence between color and brightness was inverse as one can see at Fig. 3. This means that often the construction of dependences by using *all* available data may give no useful information and, what is more, may lead to wrong conclusions. Each event in blazar's life must be considered individually.

## ACKNOWLEDGEMENTS

We thank all our colleagues who participated in observations. The research at St.-Petersburg State University is funded in part by RFBR grant 12-02-00452.

## REFERENCES

1. M. Villata, C. M. Raiteri, T. J. Balonek, *et al.*, *Astron. and Astrophys.* **453**, 817, 2006.
2. T. J. Balonek, VSNET alert circulation No. 8383, 2005.
3. V. A. Hagen-Thorn and V. A. Yakovleva, *Monthly Not. Roy. Astron. Soc.* **269**, 1069, 1994.
4. V. A. Hagen-Thorn, S. G. Marchenko, L. O. Takalo, and A. Sillanpää, *Astron. and Astrophys.* **306**, 23, 1996.
5. V. A. Hagen-Thorn, N. V. Efimova, V. M. Larionov, *et al.*, *Astr. Rep.* **53**, 510, 2009.
6. C. M. Raiteri, M. Villata, V. M. Larionov, *et al.*, *Astron. and Astrophys.* **473**, 819, 2007.
7. S. G. Jorstad, A. P. Marscher, V. M. Larionov, *et al.*, *Astrophys. J.* **715**, 362, 2010.

## RESULTS OF THE COLOR-VARIATION ANALYSIS

The flux-flux diagrams for all the data are shown in Figs. 2a and 2b for optical and IR regions separately. Fig. 2c presents the flux-flux diagram needed for joining IR and optical spectra.

One can see that the dependences between fluxes are linear. By orthogonal regression method the equations of straight lines were found as follows (in parenthesis the errors of coefficients at the level  $1\sigma$  are given, after each equation the number of points  $n$  and correlation coefficient  $r$  are given):

$$\begin{aligned} F_B &= 0.456 (\pm 0.003) F_R + 0.081 (\pm 0.016), n = 224, r = 0.998; \\ F_V &= 0.733 (\pm 0.002) F_R + 0.173 (\pm 0.013), n = 243, r = 0.996; \\ F_I &= 1.558 (\pm 0.005) F_R - 0.220 (\pm 0.026), n = 266, r = 0.996; \\ F_K &= 6.140 (\pm 0.054) F_R + 3.685 (\pm 0.357), n = 43, r = 0.937; \\ F_J &= 0.411 (\pm 0.006) F_K - 0.111 (\pm 0.216), n = 145, r = 0.981; \\ F_H &= 0.657 (\pm 0.005) F_K - 0.825 (\pm 0.190), n = 144, r = 0.993. \end{aligned} \quad (1)$$

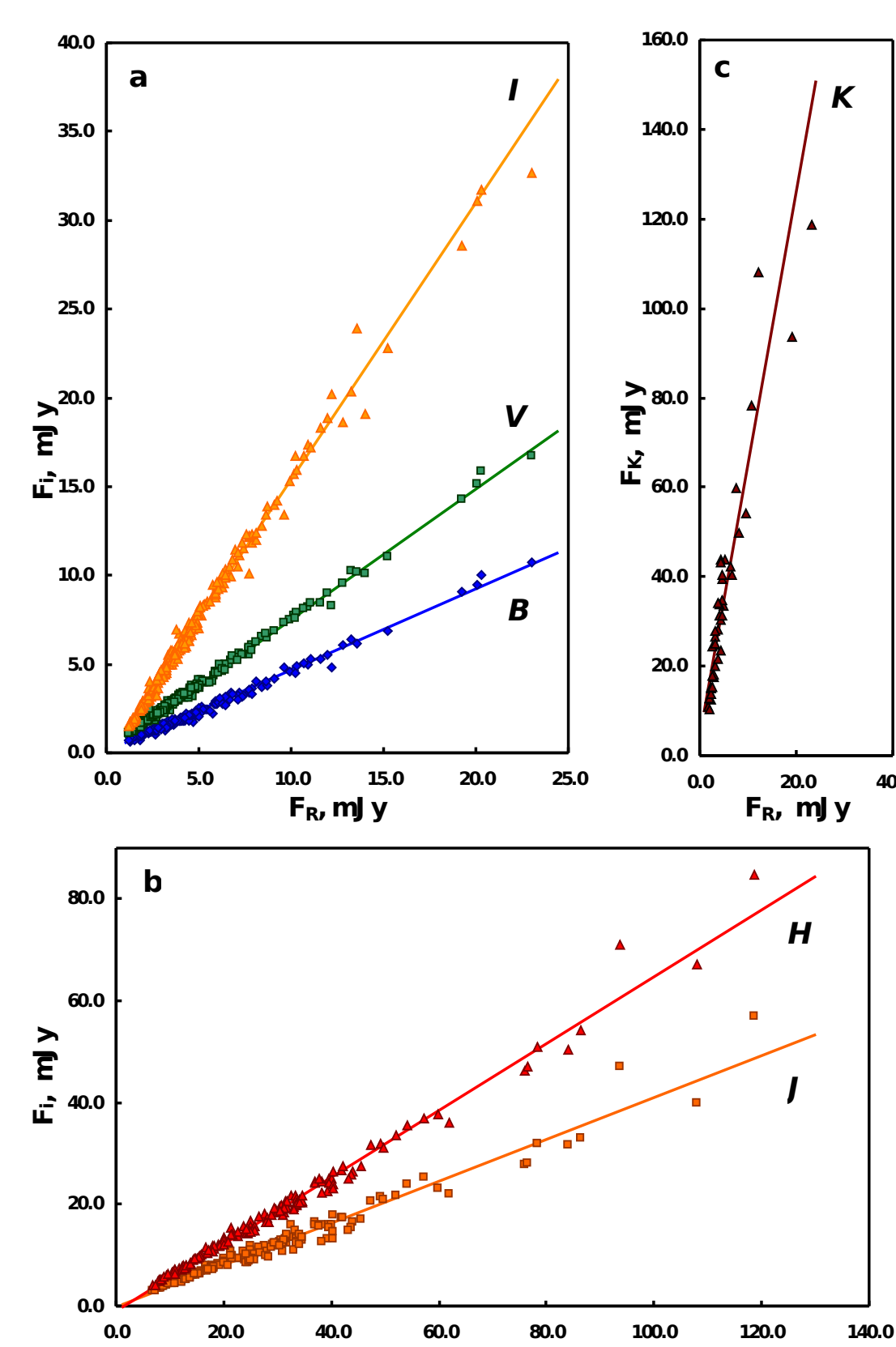


Fig. 2. “Flux-flux” diagrams

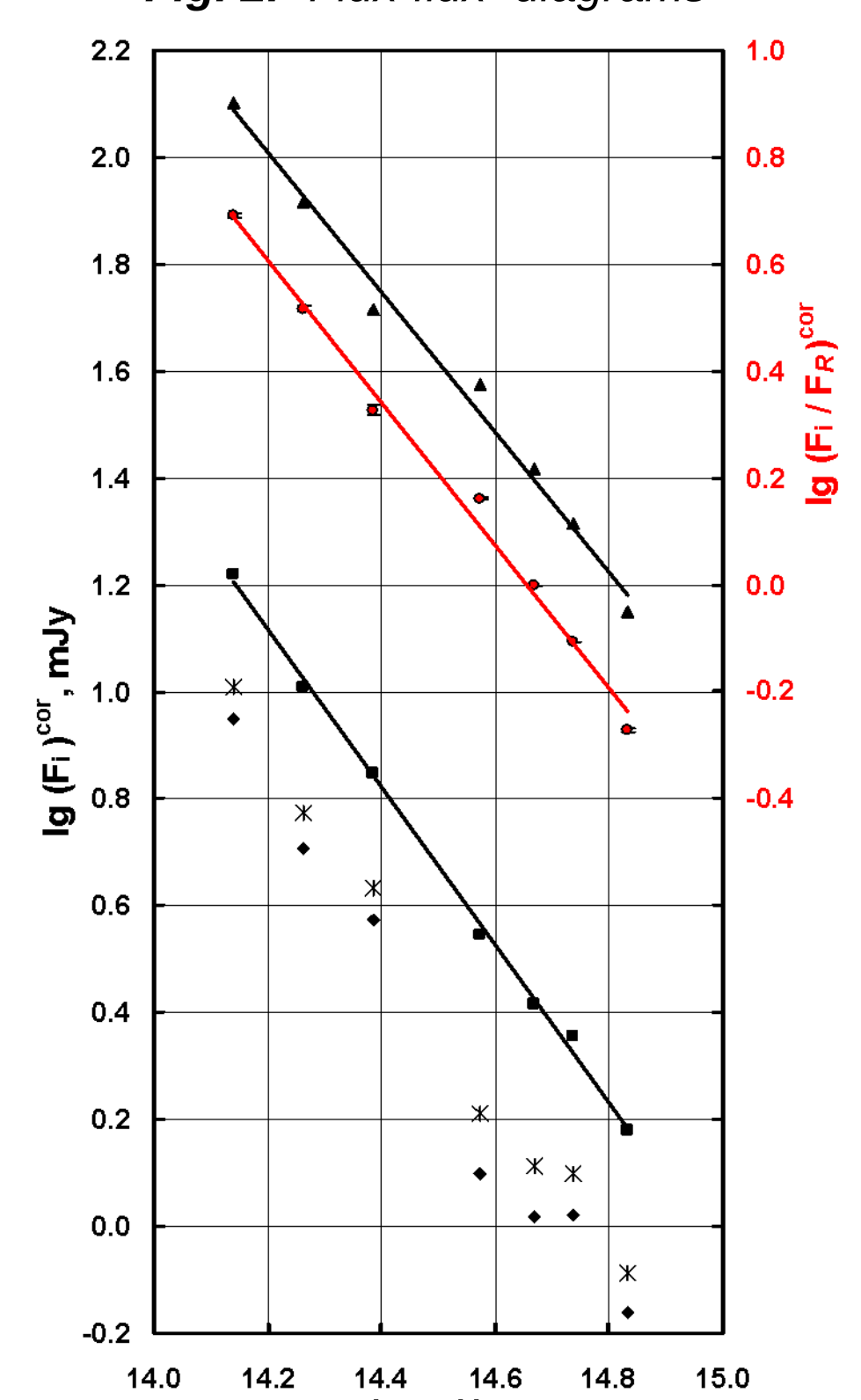


Fig.3. Relative SED of the variable component (red points with error bar, right ordinate axis) and absolute SEDs (left ordinate axis) of constant component (diamonds) and for summed radiation for different observed flux levels (asterisks, squares and triangles).

The slopes of the lines give the flux ratios of the variable component, i.e. the *mean observed* relative SED for studied time interval, while the points corresponding to constant component must lie on the straight lines nearer to coordinate origin than the points for minimum observed fluxes. All results must be corrected for interstellar extinction. This has been done as in [5].

Relative SED of the variable component, corrected for interstellar extinction, is given in logarithmic scale at Fig. 3 (red points, the right ordinate axis). One can see that SED follows the power law  $F_\nu \sim \nu^\alpha$ . Least-square fit gives the spectral index  $\alpha = -1.33 \pm 0.05$ .

Equations (1) allow to find *observed* absolute SED of the constant component, if there is an estimate of the *observed* absolute flux in one of the spectral bands. Such estimate may be found from confrontation of photometric and polarimetric observations in this band. The method is described in [11,12] and was successively used for OJ 287 in [12]. Following this method and using the results of our unpublished polarimetric observations we have found for the flux of the constant component  $F_R = 0.80$  mJy (with the uncertainty of several percents). The absolute SED of the constant component found with this value after correction for interstellar absorption is given at Fig. 3 (diamonds, left ordinate axis).

A careful examination of the flux-flux diagrams (Fig. 2) shows that the location of points seem to be represented better by segments of two straight lines with somewhat different slopes than by one line. The break is located near the value  $F_R \approx 5$  mJy ( $F_K \approx 30$  mJy). One can notice from Fig. 1 that these values lie near the upper boundary of smooth flux variations, the higher fluxes are related to outbursts.

The equations of straight lines were found separately for low ( $F_R < 5$  mJy,  $F_K < 30$  mJy) and high fluxes. The spectra in both cases are of power law. They are given at Fig. 4. The spectral indexes are  $\alpha = -1.79 \pm 0.03$  for low fluxes and  $\alpha = -1.25 \pm 0.05$  for higher fluxes so that for low fluxes the variable source is more red.

The examination of Fig. 2 shows that for high fluxes the scatter of points can hardly be explained only by observational errors. The probable reason is the difference of color characteristics of variable components responsible for outbursts. To verify this assumption the flux-flux diagrams were constructed for four time interval including outbursts: (1) JD 2454200 – 2454374, (2) JD 2454600 – 2454899, (3) JD 2454900 – 2455369, (4) JD 2455370 – 2455800. The resulting spectra are given in Fig. 5. Spectral indexes are as follows: (1)  $\alpha = -1.18 \pm 0.06$ ; (2)  $\alpha = -1.41 \pm 0.06$ ; (3)  $\alpha = -1.92 \pm 0.053$  и (4)  $\alpha = -1.68 \pm 0.06$  (for interval (3) the value of  $\alpha$  is less reliable because of lack of IR data). We see that difference of color characteristics of variable components really exists.

Fig.4. Relative SEDs for two variable sources (red points – smooth component, blue triangles – component responsible for outbursts).

Fig.5. Relative SEDs for different time intervals

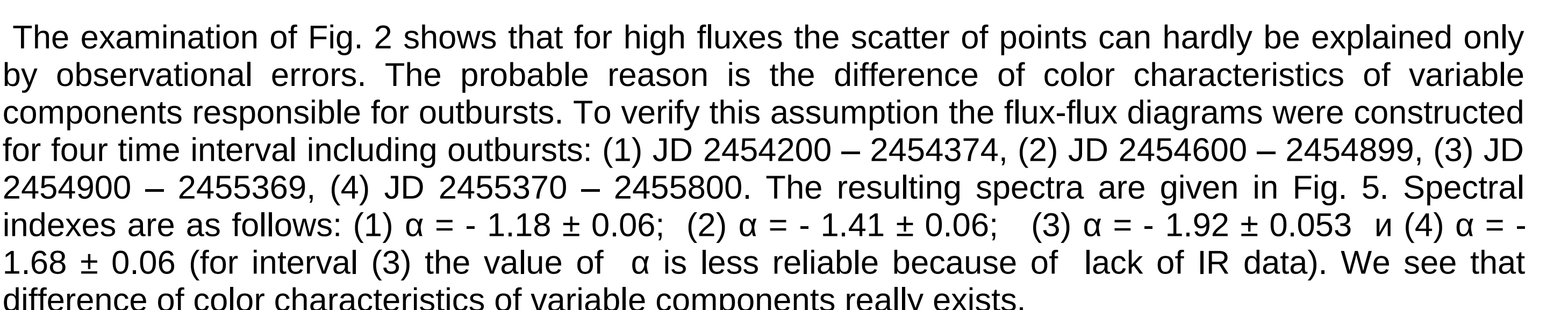


Fig.5. Relative SEDs for different time intervals

Fig.5. Relative SEDs for different time intervals

Fig.5. Relative SEDs for different time intervals

Fig.5. Relative SEDs for different time intervals

Fig.5. Relative SEDs for different time intervals

Fig.5. Relative SEDs for different time intervals

Fig.5. Relative SEDs for different time intervals

Fig.5. Relative SEDs for different time intervals

Fig.5. Relative SEDs for different time intervals

Fig.5. Relative SEDs for different time intervals

Fig.5. Relative SEDs for different time intervals

Fig.5. Relative SEDs for different time intervals

Fig.5. Relative SEDs for different time intervals

Fig.5. Relative SEDs for different time intervals

Fig.5. Relative SEDs for different time intervals

Fig.5. Relative SEDs for different time intervals

Fig.5. Relative SEDs for different time intervals

Fig.5. Relative SEDs for different time intervals

Fig.5. Relative SEDs for different time intervals

Fig.5. Relative SEDs for different time intervals

Fig.5. Relative SEDs for different time intervals

Fig.5. Relative SEDs for different time intervals

Fig.5. Relative SEDs for different time intervals

Fig.5. Relative SEDs for different time intervals

Fig.5. Relative SEDs for different time intervals

Fig.5. Relative SEDs for different time intervals

Fig.5. Relative SEDs for different time intervals

Fig.5. Relative SEDs for different time intervals

Fig.5. Relative SEDs for different time intervals

Fig.5. Relative SEDs for different time intervals

Fig.5. Relative SEDs for different time intervals

Fig.5. Relative SEDs for different time intervals

Fig.5. Relative SEDs for different time intervals

Fig.5. Relative SEDs for different time intervals

Fig.5. Relative SEDs for different time intervals

Fig.5. Relative SEDs for different time intervals

Fig.5. Relative SEDs for different time intervals

Fig.5. Relative SEDs for different time intervals